International Information and Engineering Technology Association
Advancing the World of Information and Engineering

Mathematical Modelling of an Oscillatory Flow in an Elastic Tube with Suction/Injection

Ferqunda Tabassum[1] , Muthu Poosan[1*] , J.S.V.R. Krishna Prasad[2]

[1] Department of Mathematics, National Institute of Technology, Warangal 506004, India
[2] Department of Humanities and Science, MLR Institute of Technology, Hyderabad 500043, India

Corresponding Author Email: pm@nitw.ac.in

ABSTRACT

This study presents a mathematical model of incompressible viscous fluid flow in an elastic tube with thin walls, emphasizing the function of injection or suction through the tube wall to simulate fluid exchange. Under the assumption of a minimal slope parameter, the nonlinear governing equations are linearized up to second order using a perturbation approach. For the velocity component, wall shear stress, and mean pressure drop, analytical solutions are acquired. The pressure differential equation can be solved numerically by applying Gill's fourth-order method. The tube geometry, Womersley number, suction/injection, and elasticity characteristics all have an impact on variations in wall shear stress, based on the results. Furthermore, the mean pressure drop decreases consistently with increasing elasticity value, irrespective of tube geometry.

1. INTRODUCTION

Fluid flow is a fundamental phenomenon that happens in a variety of natural and engineering systems. Viscosity, inertial forces, and external constraints are only a few of the factors that affect how fluid flows. The maintenance of the physiological characteristics of the human body depends critically on blood flow [1]. It ensures that the different tissues and organs get the needed amounts of nutrients, oxygen, and immune cells before eliminating waste from metabolism. Fluid mechanics has shown an enormous amount of interest in oscillatory flow with variable cross-sections in an elastic tube because of its importance in several physiological and engineering domains [2].

Womersley [3, 4] investigated the oscillatory movement of a viscous fluid in a thin-walled elastic tube of uniform cross-section and discovered how to use the longitudinal oscillations of the tube wall to find the volumetric flow rate. This was accomplished by using a linear approximation for long waves. By assuming the rate of reabsorption throughout the tube's length, Macey [5] developed a model to examine the viscous fluid flow in a circular tube. Rao Ramachandra [6] exploited the shell equation to generate an excess pressure equation while accounting for the flow of a viscous incompressible fluid in his research of oscillatory flow in an axially connected elastic tube with a changing cross-section. For an excess pressure, the author derived two second-order ordinary differential equations. These equations were then translated into four first-order equations, which were then numerically solved using the Runge-Kutta technique of order four. The impact of the injection/suction parameter on the fluid's pulsatile flow in a rigid circular tube with varying cross-sections was examined by Chandra and Prasad [7]. A two-dimensional nonlinear blood flow mathematical model in

tapered arteries with stenosis was developed by Chakravarthy and Mandal [8]. The authors assumed that the vascular wall's deformability is elastic and that the blood as Newtonian fluid. By employing the proper boundary conditions and the input pressure gradient resulting from the heart's periodic functioning, an analytical technique is used to compute both the axial and radial velocity profiles with minimal computer complexity.

Misra and Ghosh [9] systematically examined the flow of a viscous fluid through an elastic permeable tube with a variable cross-section in their investigation, specifically focusing on blood flow. It is also assumed that the vessel wall is tethered against longitudinal displacements. The blood is taken as Newtonian fluid in their study. As the seepage rate diminishes throughout the vessel's length, the wall is taken as porous and elastic. An analytical solution was obtained for the velocity field of pulsatile flow in a porous elastic tube with a changing cross-section. The application of the solution has been utilized to examine the impact of wall motion and wall geometry on the axial, radial velocities and mass flow. From the computational results, the authors found that the vessel wall's elasticity has a major impact on the velocity components. The significance of the slip parameter and permeability parameter on pressure drop was discussed by Das and Saha [10], taking into account the pulsatile flow of bi-viscous fluid through a rigid circular tube with suction/injection. In addition to showing that there is a rise in wall shear stress in the converging part of the tube and a reduction in the diverging region with increasing Reynolds number, their analysis found that the suction reduces shear stress and pressure drop at the tube wall. Numerous investigators have looked into pulsatile blood flow in rigid tubes with varying cross-sectional areas. However, a key factor in ensuring that blood flows through the body efficiently is the blood vessels' elastic structure,

particularly the arteries. The heart is known to pump oxygenated blood out through arteries, which ultimately split into smaller branches and supply oxygen and other nutrients to the tissues and organs [2]. Therefore, comprehension of the permeability of the artery wall is crucial to understanding the movement of nutrients.

A mathematical model of the Stokes flow of a Newtonian fluid inside a uniform porous pipe was given by Bhatti et al. [11]. After applying the similarity transformation approach to convert the governing equations into an ordinary differential equation of order three, the authors were able to solve the equations. In this investigation, the effect of small injection and suction on the velocity component was also visually shown. The influence of important physical characteristics, such as the Womersley number, Casson, and elasticity parameters, on the excess pressure fluctuation was graphically shown by Selvi and Srinivas [12]. The authors focused on non-Newtonian Casson fluid through a varying elastic tube. Particular emphasis has been placed on the pathophysiology and prevention of cardiovascular disease by Gao and Zhang [13] in their research. The derivation of a mathematical model for the nonlinear waves in an artery is presented. To explain the propagation of a viscous fluid via a thin tube, a new model of the Boussinesq equation with the viscous term is constructed, which is based on the multiscale analysis and perturbation approach. The authors investigated the influence of viscosity on the wave's amplitude and width, once the fractional equation's approximate analytical solution is found.

Manopoulos et al. [14] presented a general solution for an oscillating Stokes flow in a porous pipe. The solution is examined for various values of dimensionless parameters, such as the Womersley number and the suction/injection parameter. Shahzad [15] recently carried out an experimental study to use the inverse approach to ascertain the velocity components, wall shear stress, pressure distribution, rate of volumetric flow, pressure drop, and leakage flux. The flow of Newtonian fluid via a porous tube was taken into consideration by the author. The outcomes of two distinct scenarios involving reabsorption through channel walls were displayed. The majority of these researches took into account fluid flow with the suction/injection in a uniform cross-section. The human body contains a variety of blood vessels with different cross-sectional areas, from large arteries to tiny capillaries [16]. A more realistic representation of the physiological properties of the circulatory system can be achieved by modeling this variance.

The primary feature of blood flow in elastic tubes is considered to be its oscillating nature. The flow characteristics may be impacted by variations in the elastic tube's cross-sectional area over its length. In most of the aforementioned studies, traditional uniform cross-sections with rigid tubes have been considered. However, diameter of vessels varies with the distance as propounded by Whitmore [17]. Hence the concept of varying cross-section is the primary basis for understanding blood flow problems. It is crucial to understand the dynamics of oscillating flow in an elastic tube with different cross-sections and the effects of suction/injection in a variety of domains, including fluid dynamics.

Motivated by previous studies, we proposed a mathematical framework to investigate the oscillatory blood flow through arteries with different cross-sectional areas and permeable walls, considering the effects of injection/suction. By defining the normal velocity at the wall, the permeability of the wall is ascertained. The fluid's suction/injection velocity is

considered to oscillate with a small amplitude. This study provides a visual demonstration of the impact of various parameters on the modulus of shear stress and mean pressure drop at the tube wall, including the elastic parameter, Womersley parameter, and wall velocity (due to suction/injection).

2. PROBLEM STATEMENT

We explore an oscillatory, axially symmetric fluid flow of a Newtonian, incompressible fluid within a thin-walled, circular cross-section axi-symmetric elastic tube with suction/injection at the walls. We considered cylindrical polar coordinates (X, R, θ) to describe the elastic tube. $R=0$ is the axis and $X=0$ as the inlet of the tube. It is assumed that the elastic tube is connected against longitudinal displacements as shown in Figure 1. The radius of the tube is varying along the length of the tube, i.e., as a function of X, at each cross-section. This is written mathematically as $R=A(X)$, as the expression for the tube radius. In general,

$$A(X) = A_0 S\left(\frac{\varepsilon X}{A_0}\right) \text{ with } S(0) = 1 \qquad (1)$$

where, $\varepsilon = \frac{A_0}{L} \ll 1$ is the slope parameter of the tube wall, the radius of the tube at $X=0$ is marked by A_0 and L refers to the tube's characteristic length. Note that $\varepsilon=0$ results in the tube of uniform radius.
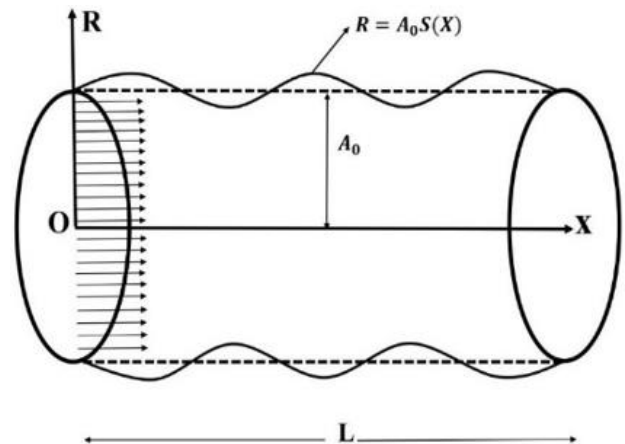
Figure 1. Geometry of the axi-symmetric, elastic tube of circular cross-section

The fundamental continuity and motion equations that regulate an axi-symmetric fluid flow are as follows:

$$\frac{\partial U}{\partial X} + \frac{\partial V}{\partial R} + \frac{V}{R} = 0 \qquad (2)$$

$$\frac{\partial U}{\partial T} + U\frac{\partial U}{\partial X} + V\frac{\partial U}{\partial R} = -\frac{1}{\rho}\frac{\partial P}{\partial X}$$
$$+\nu\left[\frac{\partial^2 U}{\partial X^2} + \frac{\partial^2 U}{\partial R^2} + \frac{1}{R}\frac{\partial U}{\partial R}\right] \qquad (3)$$

$$\frac{\partial V}{\partial T} + U\frac{\partial V}{\partial X} + V\frac{\partial V}{\partial R} = -\frac{1}{\rho}\frac{\partial P}{\partial R}$$
$$+\nu\left[\frac{\partial^2 V}{\partial X^2} + \frac{\partial^2 V}{\partial R^2} + \frac{1}{R}\frac{\partial V}{\partial R} - \frac{V}{R^2}\right] \qquad (4)$$

where, U and V indicates the axial and radial components of the fluid's velocity, P implies the pressure, ρ signifies the constant fluid density, ν indicates the kinematic viscosity coefficient and T indicates time variable.

We assumed the elastic tube to be connected against the longitudinal displacement. Consequently, the shell equation of motion for a thin elastic tube is identically satisfied as the longitudinal displacement is zero, while the equation governing radial displacement ζ due to the constriction (narrowing) of the tube at the boundary is given as [6]:

$$\frac{\partial^2 \zeta}{\partial T^2} = \frac{1}{h_1 \rho_1} \left(P - 2\nu\rho \frac{\partial V}{\partial R} \right)_{R=A(x)} - \left(\frac{B}{\rho_1} \frac{\zeta}{A^2(X)} \right) \tag{5}$$

where, h_1 and ρ_1 indicates the thickness and density of the tube material respectively and $B = \frac{E}{1-\sigma^2}$, E corresponds to Young's modulus and σ stands for Poisson's ratio [6].

The normal component of the fluid velocity at the wall of the tube is expressed as [7]:

$$V - \frac{dA}{dX} U = \left(\bar{V}_w + \frac{\partial \zeta}{\partial T} \right) \left[1 + \left(\frac{dA}{dX} \right)^2 \right]^{1/2} \text{ at } R = A(X) \tag{6}$$

Here, $\overline{V_w} = V e^{inT}$ is the oscillatory fluid velocity due to which suction/injection occurs at the permeable wall, n represents the frequency of the oscillation and $\frac{\partial \zeta}{\partial T}$ is the wall velocity due to the flexibility of the tube wall [7].

The tangential velocity at the wall is zero (no-slip condition) implies:

$$U + \frac{dA}{dX} V = 0 \text{ at } R = A(X) \tag{7}$$

The axi-symmetry of the flow is:

$$\frac{\partial U}{\partial R} = 0 \text{ and } V = 0 \text{ at } R = 0 \tag{8}$$

The flow rate $Q(X)$ is prescribed at the entrance cross-section of the tube as:

$$Q = \int_0^{A(X)} 2\pi R U \, dR = Q_0 e^{inT} \text{ at } X = 0 \tag{9}$$

where, Q_0 is a constant.

3. ANALYSIS

We introduce the following dimensionless quantities for the Eqs. (1)-(9).

$$x = \frac{\varepsilon X}{A_0}, \qquad r = \frac{R}{A_0}, \qquad t = nT, \qquad q = \frac{Q}{Q_0}$$

$$\xi = \frac{\zeta}{\varepsilon A_0}, \qquad p = \frac{\varepsilon 2 \pi A_0^3 P}{\rho \nu Q_0}$$

$$u = \frac{2\pi A_0^2 U}{Q_0}, (v, v_w) = \frac{2\pi A_0^2 (V, V_w)}{\varepsilon Q_0}$$

Thus, the Eqs. (1)-(9) reduced into the dimensionless form and expressed as below:

$$\frac{\partial u}{\partial x} + \frac{\partial v}{\partial r} + \frac{v}{r} = 0 \tag{10}$$

$$\alpha^2 \frac{\partial u}{\partial t} + \varepsilon \, Re \left[u \frac{\partial u}{\partial x} + v \frac{\partial u}{\partial r} \right] = -\frac{\partial p}{\partial x} + \varepsilon^2 \frac{\partial^2 u}{\partial x^2} + \frac{\partial^2 u}{\partial r^2} + \frac{1}{r} \frac{\partial u}{\partial r} \tag{11}$$

$$\varepsilon^2 \alpha^2 \frac{\partial v}{\partial t} + \epsilon^3 \, Re \left[u \frac{\partial v}{\partial x} + v \frac{\partial v}{\partial r} \right] = -\frac{\partial p}{\partial r} + \varepsilon^4 \frac{\partial^2 v}{\partial x^2} + \varepsilon^2 \left[\frac{\partial^2 v}{\partial r^2} + \frac{1}{r} \frac{\partial v}{\partial r} - \frac{v}{r^2} \right] \tag{12}$$

$$\varepsilon^2 H \frac{\partial^2 \xi}{\partial t^2} = \frac{1}{Re \, S t^2} \left[p - 2 \varepsilon^2 \frac{\partial v}{\partial r} \right]_{r=S(x)} - \frac{1}{\lambda^2} \frac{\xi}{S^2} \tag{13}$$

$$v - \frac{dS}{dx} u = \left(v_w e^{it} + St \frac{\partial \xi}{\partial t} \right) \left[1 + \varepsilon^2 \left(\frac{dS}{dx} \right)^2 \right]^{\frac{1}{2}}, \quad \text{at } r = S(x) \tag{14}$$

$$u + \varepsilon^2 \frac{dS}{dx} v = 0 \text{ at } r = S(x) \tag{15}$$

$$\frac{\partial u}{\partial r} = 0 \text{ and } v = 0 \text{ at } r = 0 \tag{16}$$

$$q = e^{it} \text{ at } x = 0 \tag{17}$$

where,

$$\alpha^2 = \frac{A_0^2 n}{\nu}, \ R_e = \frac{Q_0}{2\pi A_0 \nu}, \ S_t = \frac{2\pi A_0^3 n}{Q_0},$$

$$H = \frac{\rho_1 h_1}{\rho A_0} \text{ and } \lambda^2 = \frac{n^2 L^2 \rho A0}{B h_1}$$

Here, α is Womersley's number, Re is the Reynolds number, S_t is the Strouhal number, and H, λ^2 are the dimensionless numbers involved in wall properties. Parameter λ indicates the elasticity of the wall and $\lambda=0$ performs the case of rigid walls. Note that $V_w = 0$ simplifies Rao's analysis [6], in which the author considered only the zeroth order case in ε.

4. METHOD OF SOLUTION

We analyze the solution for flow variables based on the assumption of steady oscillations, as a power series stated in terms of ε:

$$F = e^{it} [F_0 + \varepsilon^2 F_2 + O(\varepsilon^4)] \tag{18}$$

where, $F(x, r, t)$ is used for any of the flow variables $u, v, p \, \xi$. Substituting the expression Eq. (18) in Eqs. (10)-(17) and considering the coefficients of the like powers of ε^0 and ε^2 by ignoring the terms of order greater than two, then the governing equations of zeroth and second-order approximations together with their respective boundary conditions are listed below.

Equations corresponding to the zeroth order in ε

$$\frac{\partial u_0}{\partial x} + \frac{\partial v_0}{\partial r} + \frac{v_0}{r} = 0 \tag{19}$$

$$\frac{\partial^2 u_0}{\partial r^2} + \frac{1}{r}\frac{\partial u_0}{\partial r} - \beta^2 u_0 = \frac{\partial p_0}{\partial x}, \tag{20}$$
$$\beta^2 = i\,\alpha^2$$

$$\frac{\partial p_0}{\partial r} = 0 \tag{21}$$

$$\xi_0 = \frac{\lambda^2 S^2}{\alpha^2 St}\,[p_0]_{r=S(x)} \tag{22}$$

$$v_0 = v_w + i\,St\,\xi_0 \text{ and } u_0 = 0, \text{ at } r = S(x) \tag{23}$$

$$\frac{\partial u_0}{\partial r} = 0 \text{ and } v_0 = 0, \text{ at } r = 0 \tag{24}$$

$$q_0 = 1, \text{ at } x = 0 \tag{25}$$

Equations corresponding to the second order in ε

$$\frac{\partial u_2}{\partial x} + \frac{\partial v_2}{\partial r} + \frac{v_2}{r} = 0 \tag{26}$$

$$\frac{\partial^2 u_2}{\partial r^2} + \frac{1}{r}\frac{\partial u_2}{\partial r} - \beta^2 u_2 = \frac{\partial p_2}{\partial x} - \frac{\partial^2 u_0}{\partial x^2} \tag{27}$$

$$\frac{\partial p_2}{\partial r} = \frac{\partial^2 v_0}{\partial r^2} + \frac{1}{r}\frac{\partial v_0}{\partial r} - \frac{v_0}{r^2} - \beta^2 v_0 \tag{28}$$

$$\xi_2 = \frac{\lambda^2 S^2}{\alpha^2 St}\left[p_2 - 2\frac{\partial v_0}{\partial r}\right]_{r=S(x)} + H\,\lambda^2 S^2\,\xi_0 \tag{29}$$

$$v_2 - \frac{dS}{dx}\,u_2 = i\,St\,\xi_2 + \frac{1}{2}(v_w + i\,St\,\xi_0)\left(\frac{dS}{dx}\right)^2, \tag{30}$$
$$\text{and } u_2 = -\frac{dS}{dx}\,v_0 \text{ at } r = S(x)$$

$$\frac{\partial u_2}{\partial r} = 0 \text{ and } v_2 = 0, \text{ at } r = 0 \tag{31}$$

$$q_2 = 0, \text{ at } x = 0 \tag{32}$$

4.1 Solution for ε^0 case

Solving the Eqs. (19)-(21) along with boundary conditions Eqs. (22)-(25), we get the solution for u_0 and v_0 as:

$$u_0 = \frac{1}{\beta^2}\frac{dp_0}{dx}\left[\frac{I_0(\beta r)}{I_0} - 1\right] \tag{33}$$

$$v_0 = \frac{-1}{\beta^2}\left[\frac{d^2 p_0}{dx^2}\left(\frac{I_1(\beta r)}{\beta I_0} - \frac{r}{2}\right) - \frac{dS}{dx}\frac{dp_0}{dx}\frac{I_1}{I_0^2}I_1(\beta r)\right] \tag{34}$$

where, $I_m(\beta r)$ denotes the modified Bessel function of order m and $I_m \equiv I_m(\beta S)$ [18].

Substituting the Eq. (33) in $q_0 = \int_{r=0}^{S(x)} r\,u_0\,dr$ which gives the zeroth order flux as:

$$q_0 = -\frac{S^2}{2\beta^2}\frac{dp_0}{dx}\frac{I_2}{I_0} \tag{35}$$

4.2 Solution for ε^2 case

After integrating Eq. (28) and using the expression Eq. (34)

for v_0, we acquire the pressure p_2, which possesses the following form:

$$p_2 = -\frac{r^2}{4}\frac{d^2 p_0}{dx^2} + f(x) \tag{36}$$

where, $f(x)$ is to be found by using the condition $p_2 = 0$, at $x = 0$.

Solving the Eqs. (26) and (27) using the Eqs. (33), (34), and (36) by substituting the corresponding boundary conditions then we obtain u_2 and v_2 as:

$$u_2 = \frac{1}{\beta^2}\left[\begin{matrix}\frac{df}{dx}\left(\frac{I_0(\beta r)}{I_0} - 1\right) + g_1(x)rI_1(\beta r) + \\ g_2(x)\,I_0(\beta r) + \frac{r^2}{4}\frac{d^3 p_0}{dx^3}\end{matrix}\right] \tag{37}$$

$$\begin{aligned} v_2 = &\ \frac{-1}{\beta^3}\left[\frac{dg_1}{dx}\,rI_2(\beta r) + \frac{dg_2}{dx}I_1(\beta r) + \frac{\beta r^3}{16}\frac{d^4 p_0}{dx^4}\right] \\ & -\frac{1}{\beta^3}\left[\frac{d^2 f}{dx^2}\left(\frac{I_1(\beta r)}{I_0}\right.\right. \\ & \left.\left. -\frac{\beta r}{2}\right) - \beta\frac{dS}{dx}\frac{I_1}{I_0^2}\frac{df}{dx}I_1(\beta r)\right] \end{aligned} \tag{38}$$

where,

$$g_1(x) = -\frac{1}{2I_0}\frac{d^3 p_0}{dx^3} + \beta\frac{dS}{dx}\frac{I_1}{I_0^2}\frac{d^2 p_0}{dx^2} + \frac{g_3(x)}{2\,I_0^2}\frac{dp_0}{dx} \tag{39}$$

$$\begin{aligned} g_2(x) = &\ \frac{d^3 p_0}{dx^3}\left(\frac{S\,I_1}{2I_0^2} - \frac{S^2}{4\,I_0}\right) - \frac{d^2 p_0}{dx^2}\left(\begin{matrix}\frac{S\,I_2}{2\,I_0^2}\frac{dS}{dx} \\ +S\beta\frac{dS}{dx}\frac{I_1^2}{I_0^3}\end{matrix}\right) \\ & -\frac{dp_0}{dx}\left[\left(\frac{dS}{dx}\right)^2\frac{I_1^2}{I_0^3} - \frac{S\,I_1}{2\,I_0^3}g_3(x)\right] \end{aligned} \tag{40}$$

where,

$$\begin{aligned} g_3(x) = &\ \beta\frac{d^2 S}{dx^2}I_1 + \beta\left(\frac{dS}{dx}\right)I_1' - \\ & 2\beta^2\left(\frac{dS}{dx}\right)^2\frac{I_1^2}{I_0}, \text{ and } I_1' = \frac{d}{dx}\{I_1(\beta s)\} \end{aligned} \tag{41}$$

Substituting the Eq. (37) in $q_2 = \int_{r=0}^{S(x)} r\,u_2\,dr$, then we obtain the expression for flux q_2 as:

$$q_2 = \frac{1}{\beta^2}\left[-\frac{S^2\,I_2}{2\,I_0}\frac{df}{dx} + \frac{S^2}{\beta}I_2\,g_1 + \frac{S\,I_1}{\beta}g_2 + \frac{S^4}{16}\frac{d^3 p_0}{dx^3}\right] \tag{42}$$

Substituting the expressions for p_2, v_0, and ξ_0 in Eq. (29), we get ξ_2 as:

$$\begin{aligned} \xi_2 = &\ \frac{S^2\,\lambda^2}{\alpha^2\,S_t}\left[-\frac{S^2}{4}\frac{d^2 p_0}{dx^2} + f(x) + \right. \\ & \frac{2}{\beta^2}I_1'\left(\frac{1}{\beta I_0}\frac{d^2 p_0}{dx^2} - \frac{I_1}{I_0^2}\frac{dS}{dx}\frac{dp_0}{dx}\right) \\ & \left. -\frac{1}{\beta^2}\frac{d^2 p_0}{dx^2} + \lambda^2\,H\,S^2\,p_0\right] \end{aligned} \tag{43}$$

Now, to obtain the equation governing pressure, we put the expressions of v_0 and ξ_0 in the condition (23), and we get:

$$\frac{d^2p_0}{dx^2} + a(\beta s)\frac{dp_0}{dx} + b(\beta s)\,p_0 = c(\beta s) \qquad (44)$$

where,

$$a(\beta s) = 2\frac{dS}{dx}\frac{I_1^2}{SI_0\,I_2},$$
$$b(\beta s) = 2\,S\,\lambda^2\frac{I_0}{I_2}, c(\beta s) = 2\,\beta^2\,v_w\frac{I_0}{S\,I_2}$$

The initial conditions for p_0 are prescribed as:

$$\overline{p_0} = p_{in} = 1 \text{ and } \frac{dp_0}{dx} = -2\,\beta^2\frac{I_0}{I_2}, \text{at } x = 0 \qquad (45)$$

Substituting the expressions (38) and (43) for v_2 and ξ_2 in the condition (30) for determining $f(x)$ as:

$$\frac{d^2f}{dx^2} + a(\beta s)\frac{df}{dx} + b(\beta s)\,f = d(\beta s) \qquad (46)$$

where,

$$d(\beta s) = -2S\lambda^2\frac{I_0}{I_2}\,[-\frac{d^2p_0}{dx^2}(\frac{S^2}{4} + \frac{1}{\beta^2}) +$$
$$\frac{2}{\beta^2 I_0}\,I_1'\,(\frac{1}{\beta}\frac{d^2p_0}{dx^2} - \frac{dS}{dx}\frac{I_1}{I_0}\frac{dp_0}{dx})H\,\lambda^2\,S^2\,p_0\,]$$
$$+\frac{2I_0}{\beta\,S\,I_2}\,[SI_2\frac{dg_1}{dx} + I_1\frac{dg_2}{dx} + \frac{\beta\,S^3}{16}\frac{d^4p_0}{dx^4}]$$
$$+\frac{I_0\,\beta^2}{S\,I_2}\,(\frac{dS}{dx})^2\,[v_w + i\frac{\lambda^2\,S^2}{\alpha^2}p_0]$$
$$+\frac{2\,I_0}{I_2}\,[I_1\,g_1\frac{dS}{dx} + \frac{I_0}{S}\,g_2\frac{dS}{dx} + \frac{S}{4}\frac{dS}{dx}\frac{d^3p_0}{dx^3}] \qquad (47)$$

From Eqs. (36) and (42), the associated initial conditions are obtained as follows:

$$f(x) = \frac{1}{4}\frac{d^2p_0}{dx^2}$$
$$\frac{df}{dx} = \frac{2\,I_0}{\beta\,I_2}\,[I_2\,g_1 + I_1\,g_2 + \frac{\beta}{16}\frac{d^3p_0}{dx^3}], \qquad (48)$$
$$\text{at } x = 0$$

The differential Eq. (44) for $p_0(x)$ and the Eq. (46) for $f(x)$ are solved numerically with the corresponding initial conditions using Gill's method. Then the modulus p_{mean} is:

$$p_{mean} | = \left\{ \begin{array}{l} [\,(p_0 + \varepsilon^2\,p_2\,)_{re}\,]^2 + \\ [\,(p_0 + \varepsilon^2\,p_2\,)_{im}\,]^2 \end{array} \right\}^{1/2} \qquad (49)$$

The mean pressure drop is:

$$\Delta p = p_{mean} - p_{in} \qquad (50)$$

Wall shear stress: The non-dimensional wall shear stress T_w is [7]:

$$T_w = \frac{2\pi A_0^3\tau_w}{\rho v Q_0} = e^{it}\,\left\{\frac{\partial u_0}{\partial r}\right.$$
$$+ \varepsilon^2\,\left[\frac{\partial u_2}{\partial r} - 2\left(\frac{dS}{dx}\right)^2\frac{\partial u_0}{\partial r} + \frac{\partial v_0}{\partial x}\right.$$
$$\left.\left. - \frac{2}{r}\frac{dS}{dx}\,v_0 - 4\frac{dS}{dx}\frac{\partial u_0}{\partial x}\right]\right\} + O(\varepsilon^4) \qquad (51)$$

$$= e^{it}\,[T_{0w} + \varepsilon^2 T_{2w}] + O(\varepsilon^4)$$

where,

$$T_{0w} = \frac{1}{\beta}\frac{I_1}{I_0}\frac{dp_0}{dx} \qquad (52)$$

$$T_{2w} = \frac{4}{\beta}\left(\frac{dS}{dx}\right)^2\frac{I_1}{I_0}\frac{dp_0}{dx} - \frac{2}{S}\frac{dS}{dx}\left[v_w\right.$$
$$\left. + i\frac{\lambda^2\,S^2}{\alpha^2}p_0\right] + \frac{1}{\beta^2}\,g_4(x) + \frac{dp_0}{dx}\frac{I_1}{\beta^2}\,g_5(x)$$
$$+ \frac{I_1}{\beta\,I_0}\frac{df}{dx} + \frac{S\,I_0}{\beta}\,g_1(x)$$
$$+ \frac{I_1}{\beta}\,g_2(x) + \frac{S}{2\,\beta^2}\frac{d^3p_0}{dx^3} \qquad (53)$$

where,

$$g_4(x) = \frac{S\,I_2}{2\,I_0}\frac{d^3p_0}{dx^3} + 2\frac{dS}{dx}\frac{I_1^2}{I_0^2}\frac{d^2p_0}{dx^2} \qquad (54)$$

$$g_5(x) = \frac{I_1}{I_0^2}\frac{d^2S}{dx^2} + \frac{dS}{dx}\frac{d}{dx}\left(\frac{I_1}{I_0^2}\right) - \frac{2}{\beta\,I_0}\left(\frac{dS}{dx}\right)^2 \qquad (55)$$

Now the modulus of wall shear stress is:

$$|\,T_w\,| = \left(T_{re}^2 + T_{im}^2\right)^{1/2} \qquad (56)$$

where, T_{re} and T_{im} represents the real and imaginary parts of obtained using the Eqs. (51)-(55).

5. RESULTS AND DISCUSSION

The formulations for the modulus of wall shear stress $|T_w|$ from Eq. (56) and the mean pressure drop Δp from Eq. (50) are numerically evaluated with the corresponding initial conditions using Gill's method of order 4 and plotted in the Figures 2-9 and 10-15 respectively. Womersley parameter α value between 3 and 10 can be relevant to various arteries within the human cardiovascular system. This range indicates that the flow in the artery exhibits a balance between inertial and viscous effects, with moderate levels of pulsatility [1]. The results are obtained by taking $\varepsilon = 0.05$, $H = 0.055$, $\alpha = 4, 10$, $\lambda = 0, 0.25, 0.5$ and $v_w = -0.4, 0.0, 0.4$, references [1, 7] for the tube geometries described below:

(i) Convergent tube: $S(x) = e^{-0.1x}$.
(ii) Divergent tube: $S(x) = e^{0.1x}$.
(iii) Locally Constricted tube: $S(x) = \left[4 - e^{-(x-0.5)^2}\right]/(4 - e^{-0.25})$.
(iv) Sinusoidal tube: $S(x) = 1 + 0.2\,sin(2\pi x)$.

Here, x vs. $|T_w|$ and x vs. Δp are plotted in the Figures 2-9 and 10-15 respectively. It is observed that the expressions for $|T_w|$ and Δp depends on the dimensionless parameters such as α (Womersley parameter), λ (elasticity parameter), v_w (velocity at the wall).

5.1 Magnitude of wall shear stress

5.1.1 Convergent tube
The profile of $|T_w|$ is illustrated in Figures 2 and 3 for a convergent tube with α values 4 and 10. Suction diminishes

the flow within the tube which reduces the wall shear stress and it is depicted in Figures 2 and 3. These values are less in the case of suction $v_w = 0.4$ when compared to the corresponding values in the case of injection $v_w = -0.4$.

and injection ($v_w = -0.4$) cases.
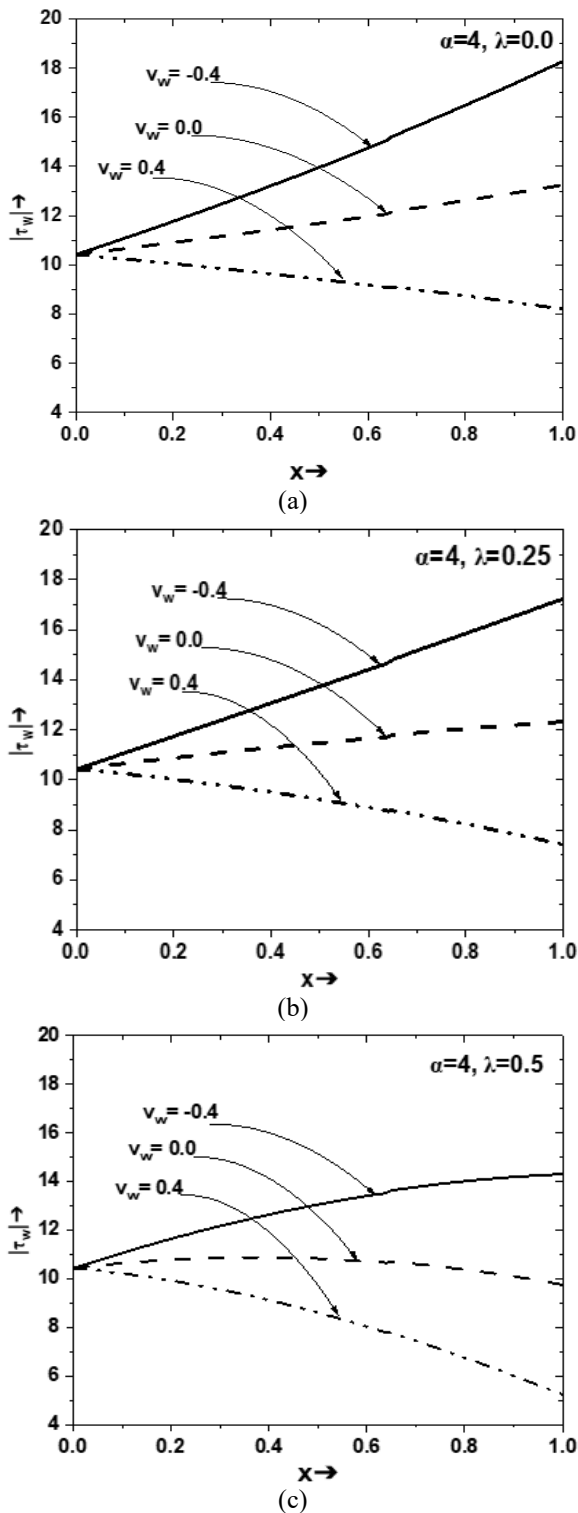
Figure 2. $|T_w|$ vs. x for convergent tube for $\alpha = 4$ in case of (a) λ=0, (b) λ =0.25, (c) λ =0.5

(a)

(b)

(c)

Figure 3. $|T_w|$ vs. x for convergent tube for $\alpha = 10$ in case of (a) λ=0, (b) λ =0.25, (c) λ =0.5

In the case of a rigid tube wall (λ=0), the wall does not deform significantly under the influence of fluid flow. As a result, the $|T_w|$ is higher at λ =0.0 when compared to the case of elastic tube wall (λ=0.25) and as λ value increases from 0.25 to 0.5, the values of $|T_w|$ decrease very fast. As α increases, the value of $|T_w|$ increases in both suction (v_w= 0.4)

5.1.2 Divergent tube

Figures 4 and 5 exhibit how the wall shear stress $|T_w|$ varies in the case of a diverging tube for distinct values of α.

In general, a higher α value indicates a stronger influence of inertia on the flow, which leads to larger fluctuations in the velocity and pressure during the pulsatile flow. These velocity fluctuations result in higher wall shear stress magnitudes. $|T_w|$ increases slowly as α increases from 4 to 10 and it is shown in Figures 4 and 5.
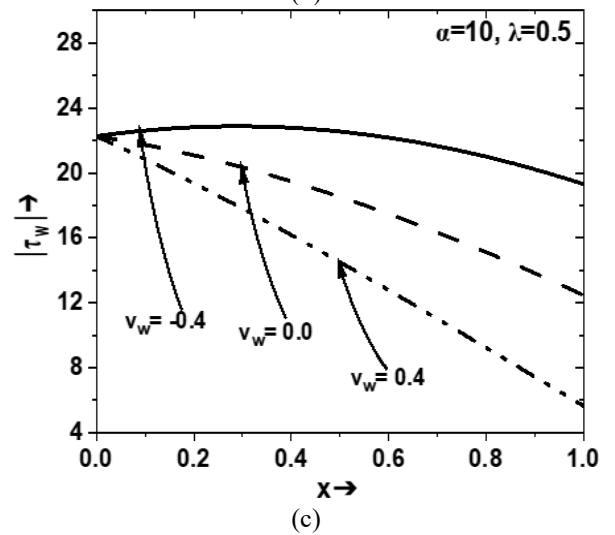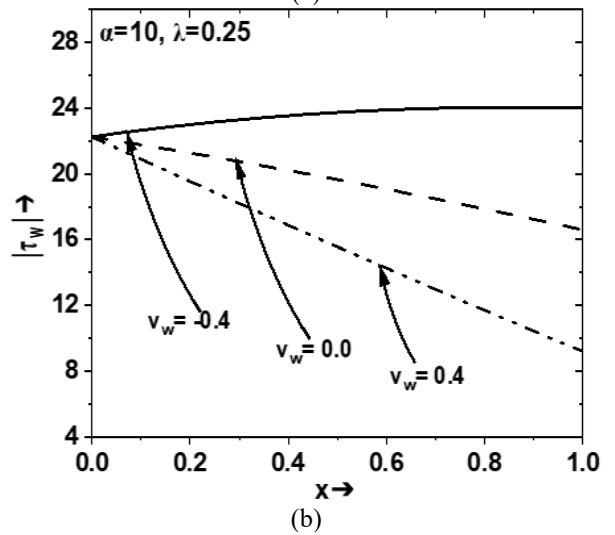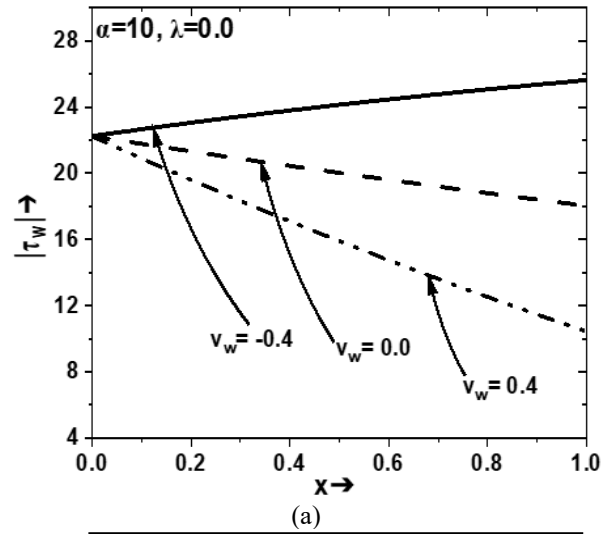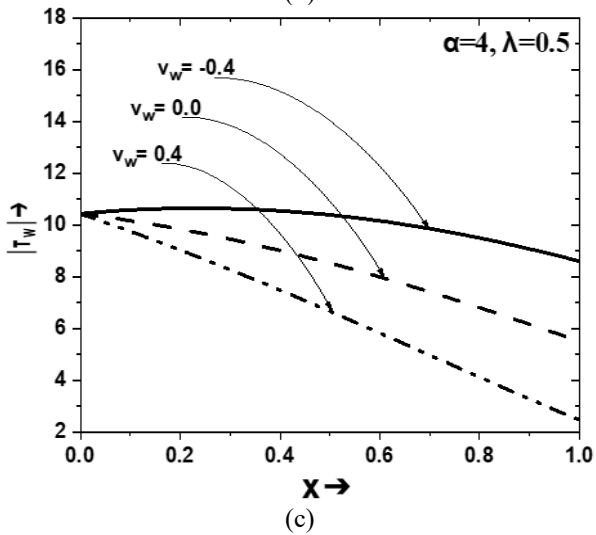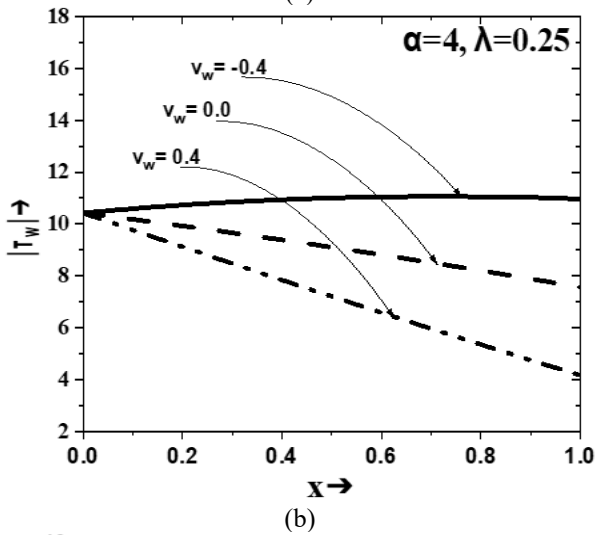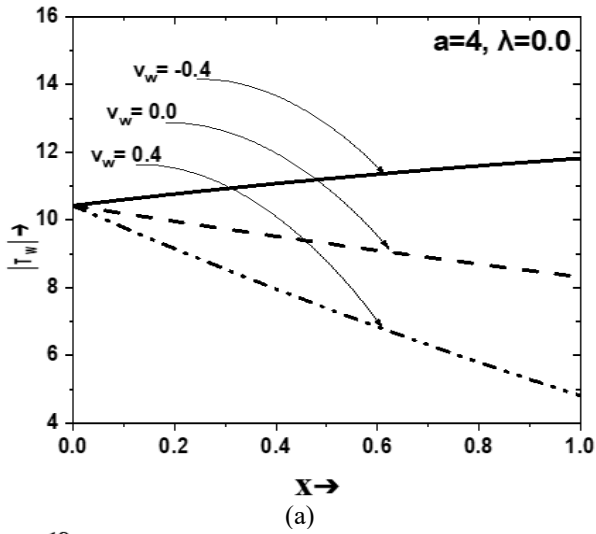
Figure 4. $|T_w|$ vs. x for divergent tube for $\alpha = 4$ in case of (a) λ=0, (b) λ =0.25, (c) λ =0.5

Figure 5. $|T_w|$ vs. x for divergent tube for $\alpha = 10$ in case of (a) λ =0, (b) λ =0.25, (c) λ =0.5

When the tube wall is elastic, it can deform under the influence of fluid flow. If the elastic wall is highly deformable, it can absorb some of the shear stress energy by deforming and expanding under the influence of fluid flow. This leads to a reduction of $|T_w|$. The walls act as buffers by absorbing and redistributing the shear stress, which reduces the size of the shear stress of the elastic wall compared to the rigid wall. Thus, as λ value increases, the values of $|T_w|$ decrease slowly in both suction and injection cases.

5.1.3 Locally constricted tube

In Figures 6 and 7, the profile of wall shear stress $|T_w|$ is portrayed for a locally constricted tube for various Womersley parameter values.

In locally constricted tubes, the $|T_w|$ can exhibit complex behavior. The presence of constrictions can create flow disturbances, separation leading to variations in the wall shear stress magnitude. In some cases, the constrictions can lead to increased wall shear stress due to flow acceleration while in

others, it can reduce wall shear stress modulus.

It is observed from Figures 6 and 7, that the values of $|T_w|$ increase between the cross-section $x = 0$ and 0.6, then decrease continuously in case of injection. But in the case of suction, the values start decreasing from $x = 0.3$ only. As α increases, the values of $|T_w|$ increase in both suction ($v_w = 0.4$) and injection ($v_w = -0.4$) cases, and also as λ value increases, the values of $|T_w|$ decreases as shown in Figures 6 and 7.
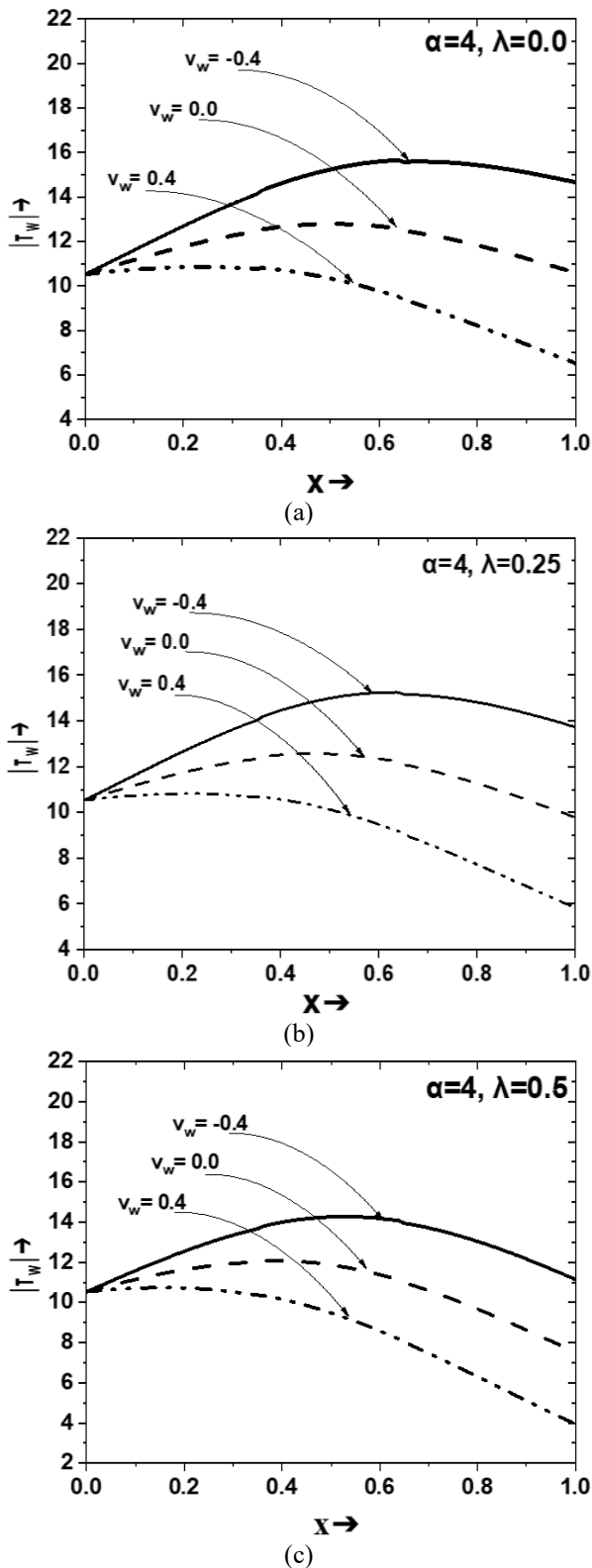
Figure 6. $|T_w|$ vs. x for locally constricted tube for $\alpha = 4$ in case of (a) $\lambda = 0$, (b) $\lambda = 0.25$, (c) $\lambda = 0.5$
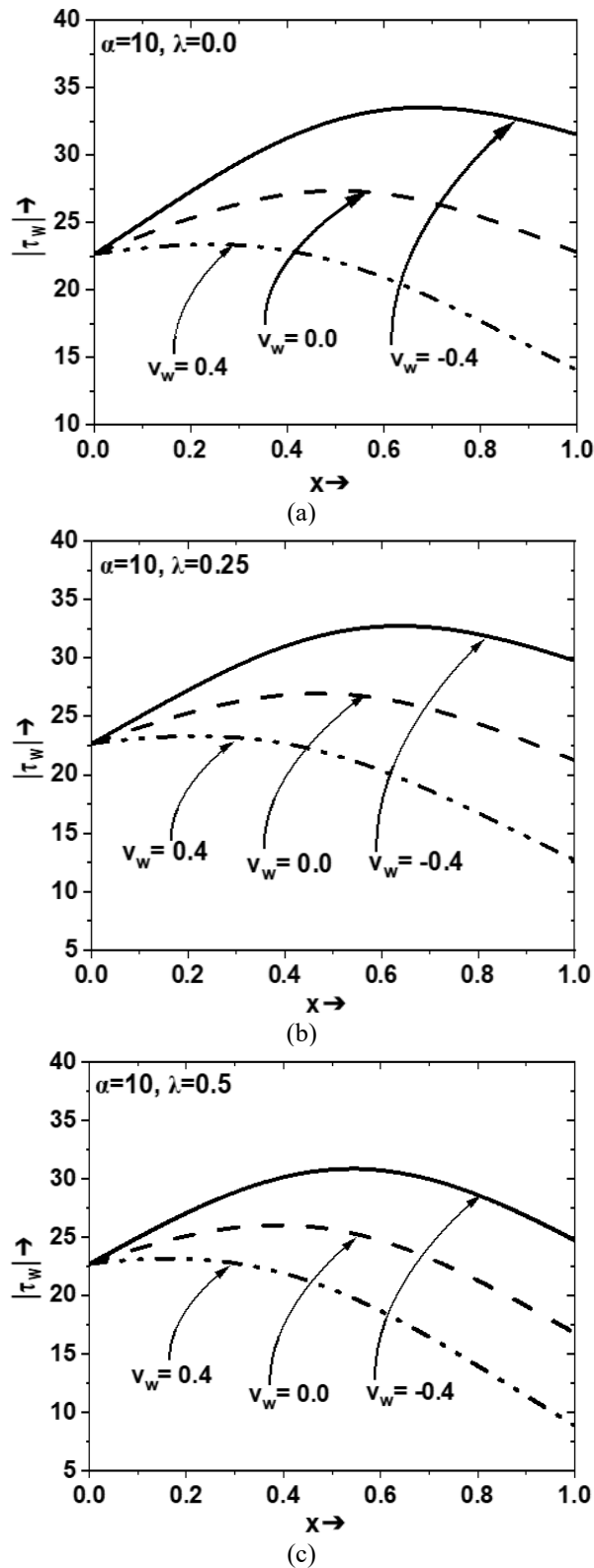
Figure 7. $|T_w|$ vs. x for locally constricted tube for $\alpha = 10$ in case of (a) $\lambda = 0$, (b) $\lambda = 0.25$, (c) $\lambda = 0.5$

5.1.4 Sinusoidal tube

Figures 8 and 9 visually show the distribution of $|T_w|$ for a sinusoidal tube with α values 4 and 10 respectively.

In a sinusoidal tube geometry, the $|T_w|$ can vary along the tube length due to the difference between the contraction and expansion region. The wall shear stress modulus increases in the localized constriction, whereas the expansion region causes a decrease in the wall shear stress modulus.

We experienced that the oscillation's amplitude increases

more sharply as α increases from 4 to 10. A high α value indicates that the oscillatory flow is dominated by inertia. It means the flow is more pulsatile, and the fluid accelerates and decelerates more rapidly as it flows within the tube. In an elastic tube with suction/injection, the changing cross-sectional area and rapid oscillations lead to variations in $|T_w|$. As α increases, these variations become more significant.

Therefore, the effect of the Womersley parameter is greater in sinusoidal tubes than in other geometries as shown in Figures 8 and 9. As λ value increases, $|T_w|$ values decrease slowly in suction/injection cases.

Hence from the above analysis, we can conclude that the amount of rise or fall in $|T_w|$ depends on, not only α and λ but also the geometry of the tube we are considering.
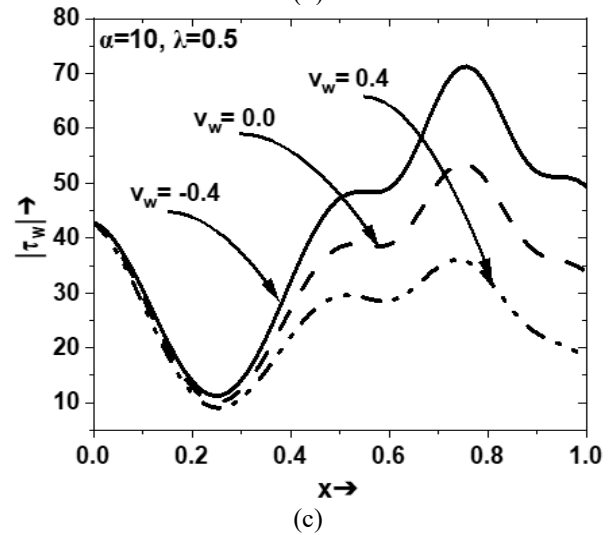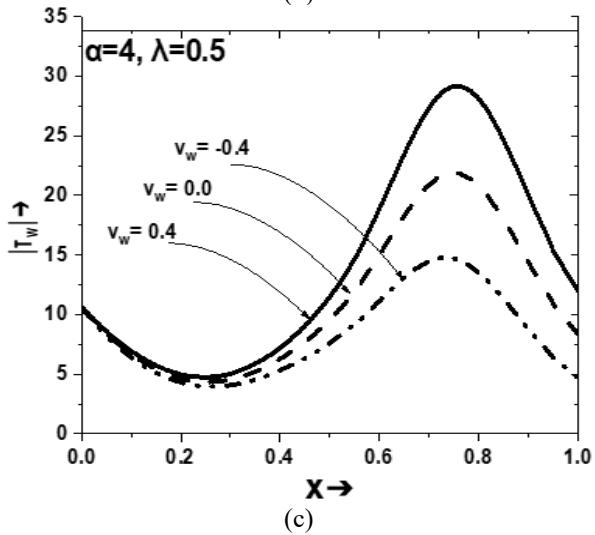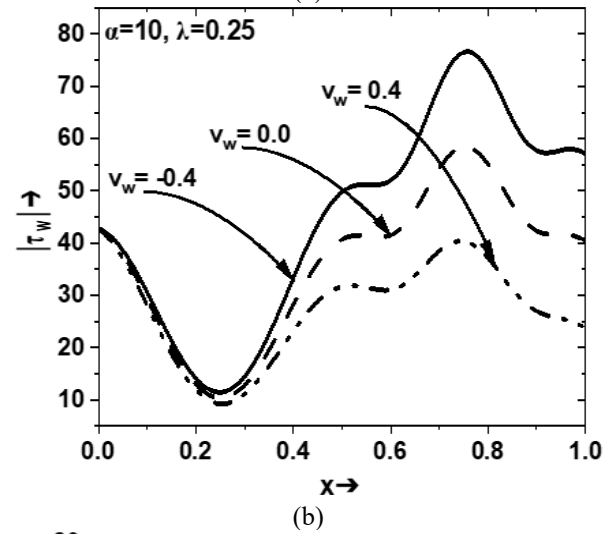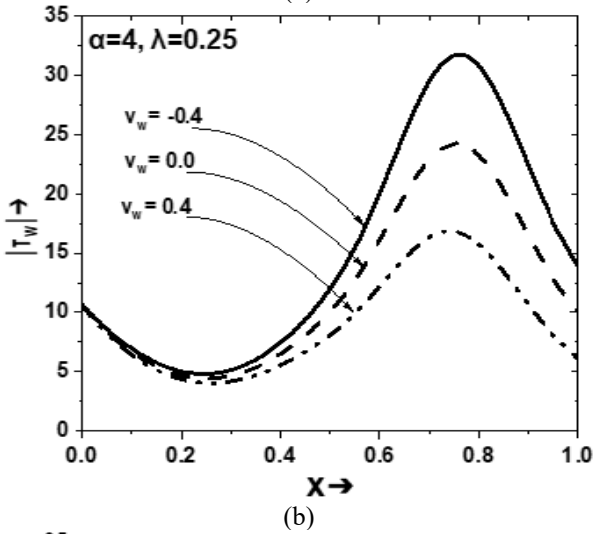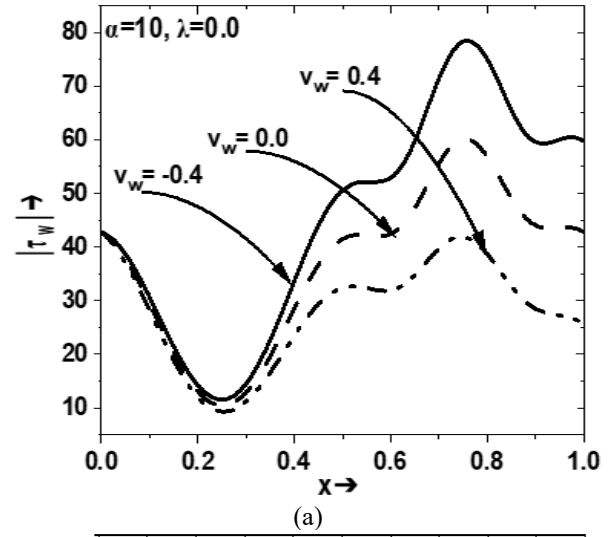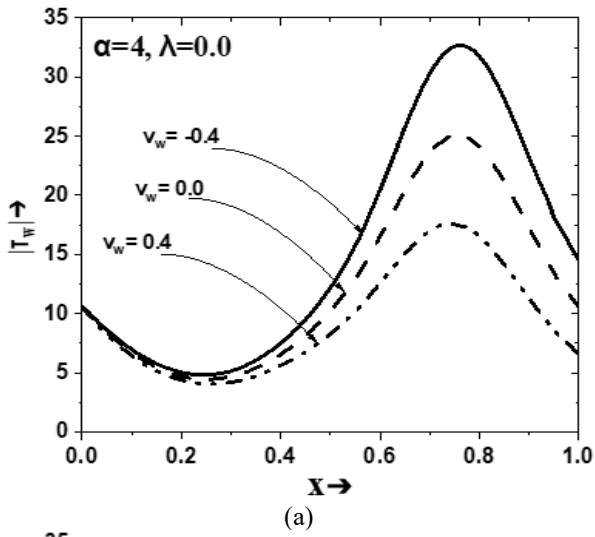
Figure 8. $|T_w|$ vs. x for sinusoidal tube for $\alpha = 4$ in case of (a) $\lambda = 0$, (b) $\lambda = 0.25$, (c) $\lambda = 0.5$

Figure 9. $|T_w|$ vs. x for sinusoidal tube for $\alpha = 10$ in case of (a) $\lambda = 0$, (b) $\lambda = 0.25$, (c) $\lambda = 0.5$

5.2 Mean pressure drop

5.2.1 Convergent tube

The impact of various parameters on mean pressure drop Δp for a convergent tube is shown in Figures 10 and 11.

(a)

(b)

(c)
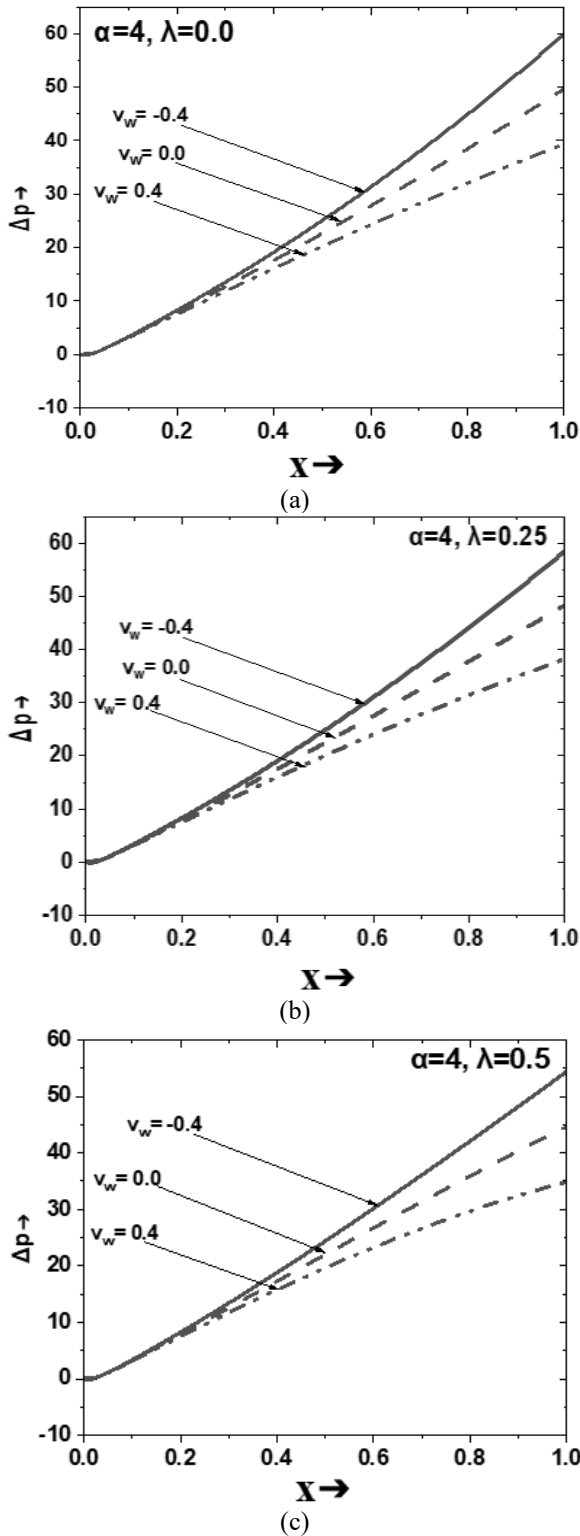
Figure 10. Δp vs. x for convergent tube for $\alpha = 4$ in case of (a) $\lambda = 0$, (b) $\lambda = 0.25$, (c) $\lambda = 0.5$

As α increases, the flow becomes more dynamic and exhibits stronger oscillatory behavior. This increased pulsatility can result in a higher Δp. The fluctuations in velocity and pressure during each oscillation cycle introduce additional flow resistance, leading to an increased pressure drop, which is shown in Figures 10 and 11 in the case of the convergent tube. And also, as the elasticity parameter λ value increases, the values of Δp decrease slowly. The values of Δp are less in the case of suction $v_w = 0.4$ when compared to the corresponding values of Δp in the case of injection $v_w = -0.4$.

It is crucial to acknowledge that similar outcomes are observed when a tube is locally constricted. For this reason, this study does not include the presentation of graphs depicting the relationship between x and Δp for the locally constricted tube case.

(a)

(b)

(c)
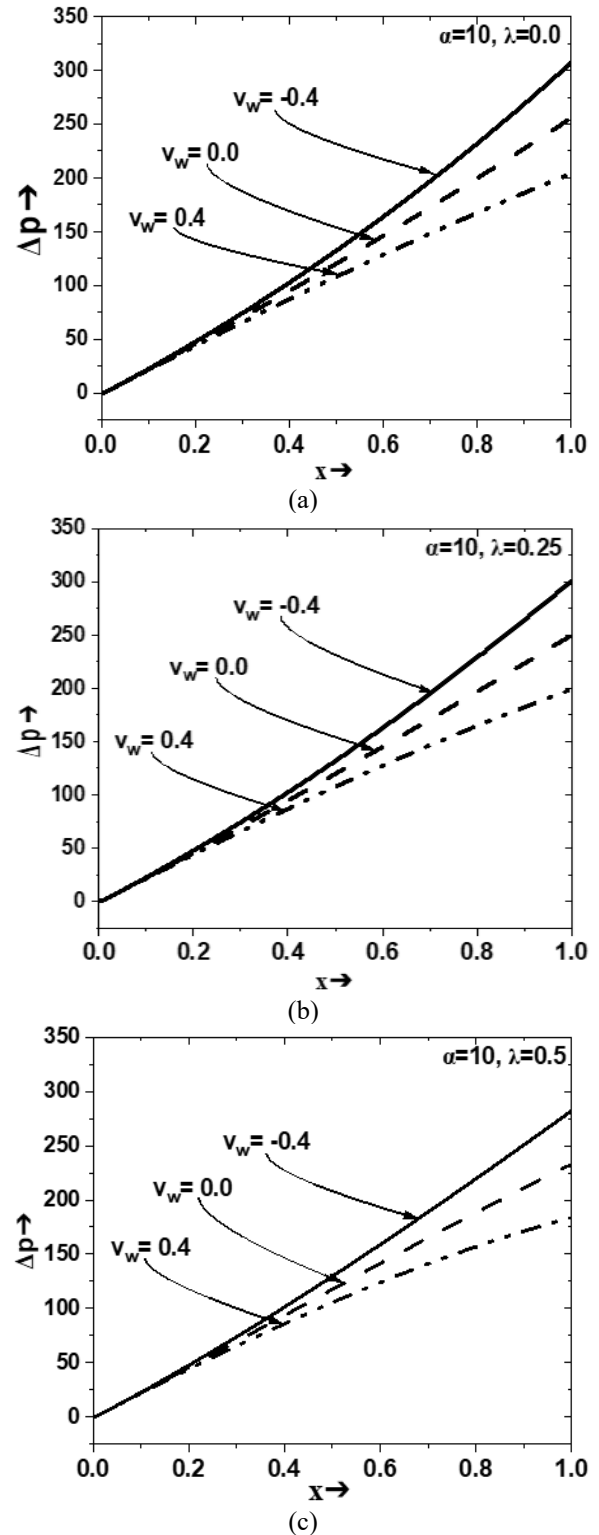
Figure 11. Δp vs. x for convergent tube for $\alpha = 10$ in case of (a) $\lambda = 0$, (b) $\lambda = 0.25$, (c) $\lambda = 0.5$

5.2.2 Divergent tube

Figures 12 and 13 are plotted to depict the effects of various values of Womersley parameter α, elasticity parameter λ, including suction/injection velocity parameter v_w.

(a)

(b)

(c)
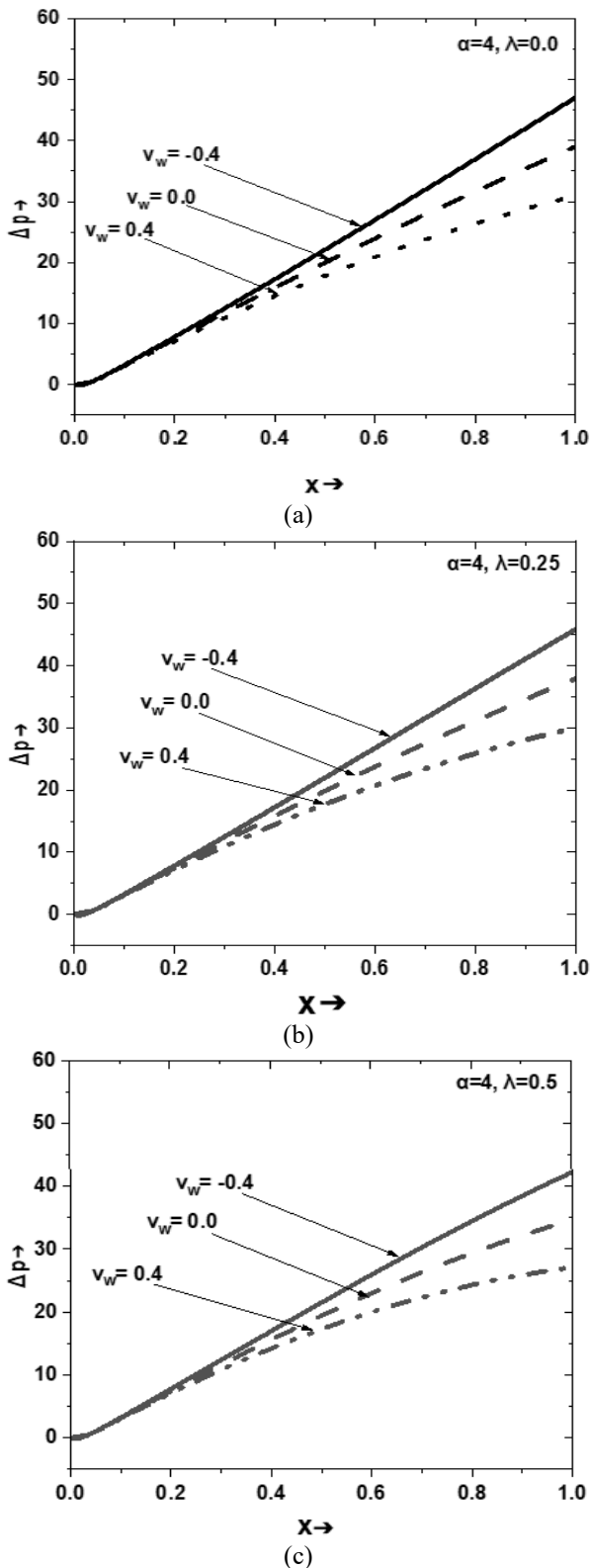
Figure 12. Δp vs. x for divergent tube for $\alpha = 4$ in case of (a) λ=0, (b) λ =0.25, (c) λ =0.5

In divergent tubes, the values of Δp are high in the case of Injection when compared to the case of Suction. The mean pressure drop values decrease as λ increases, as shown in Figures 12 and 13.

(a)

(b)

(c)
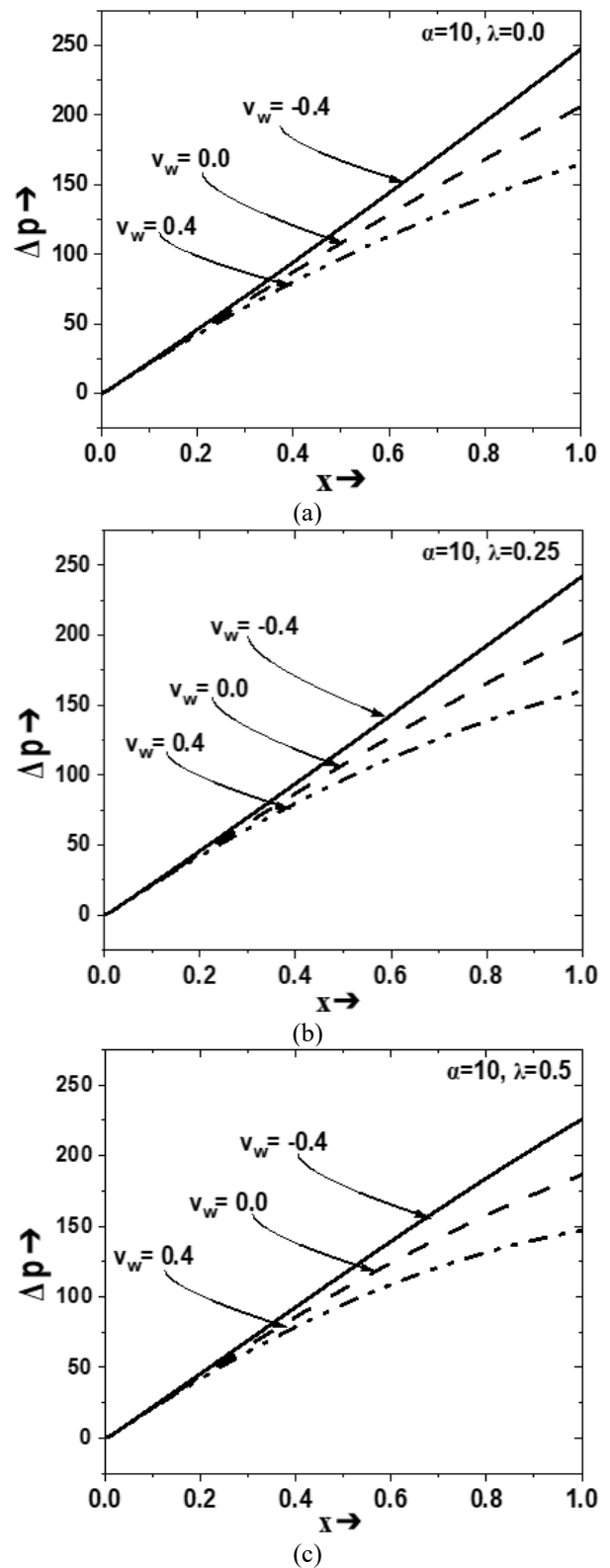
Figure 13. Δp vs. x for divergent tube for $\alpha = 10$ in case of (a) λ =0, (b) λ =0.25, (c) λ =0.5

As α rises, there is an associated increase in the Δp due to the more significant variations in pressure during the flow cycle, particularly within the divergent tube as shown in Figures 12 and 13. Additionally, we noticed that in comparison to the analogous values of Δp in the condition of injection v_w = -0.4, the values of Δp are lower in the case of suction v_w = 0.4.

5.2.3 Sinusoidal tube

To check the impact of various parameters on Δp for a sinusoidal tube, we plotted Figures 14 and 15.

(a)

(b)

(c)
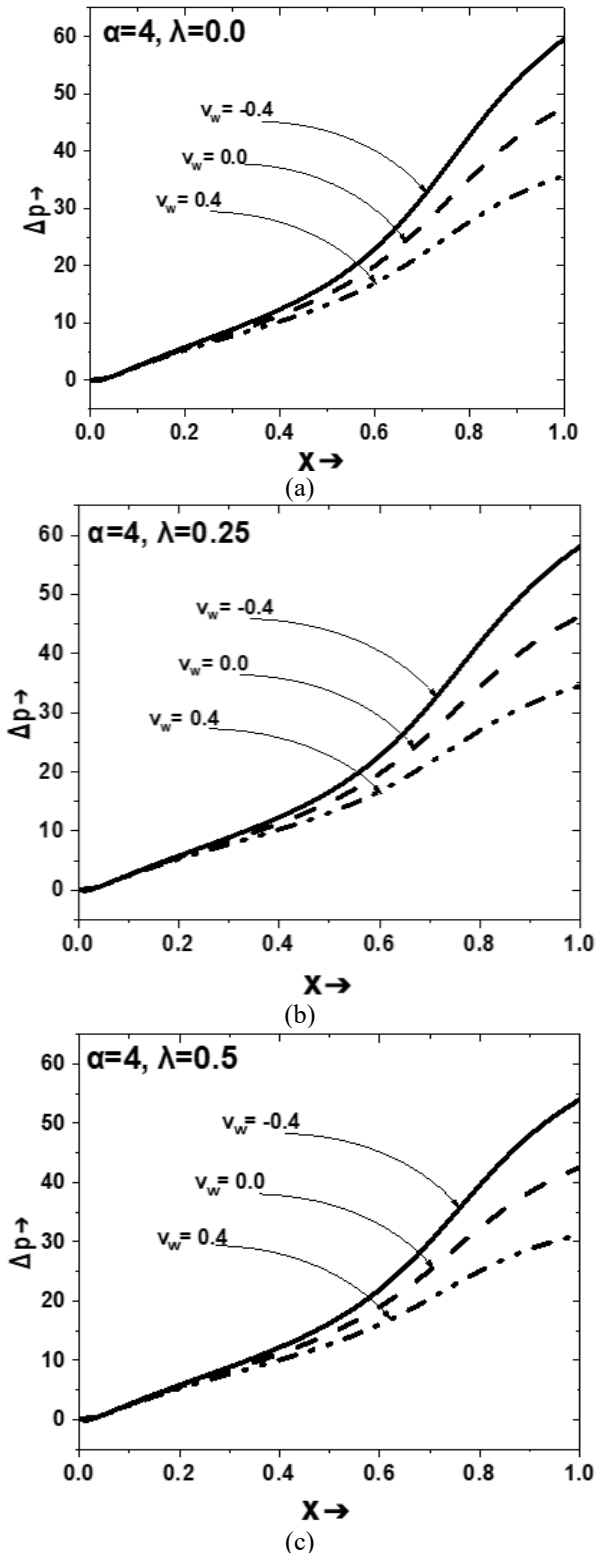
Figure 14. Δp vs. x for sinusoidal tube for $\alpha = 4$ in case of (a) λ =0, (b) λ =0.25, (c) λ =0.5

In the case of a sinusoidal tube, Δp values exhibit a gradual increase, as x moves from 0.0 to 0.6. However, there is a rapid increase in Δp values, when x ranges from 0.6 to 1.0, both in the case of suction and injection as shown in Figures 14 and 15.

This interesting behavior is observed which is different from the other three geometries. As α increases, Δp values in

a sinusoidal tube with an oscillatory flow in an elastic tube of varying cross-section with suction/injection is likely to increase from 60 to 300, due to the more significant variations in pressure during the flow cycle.

(a)

(b)

(c)
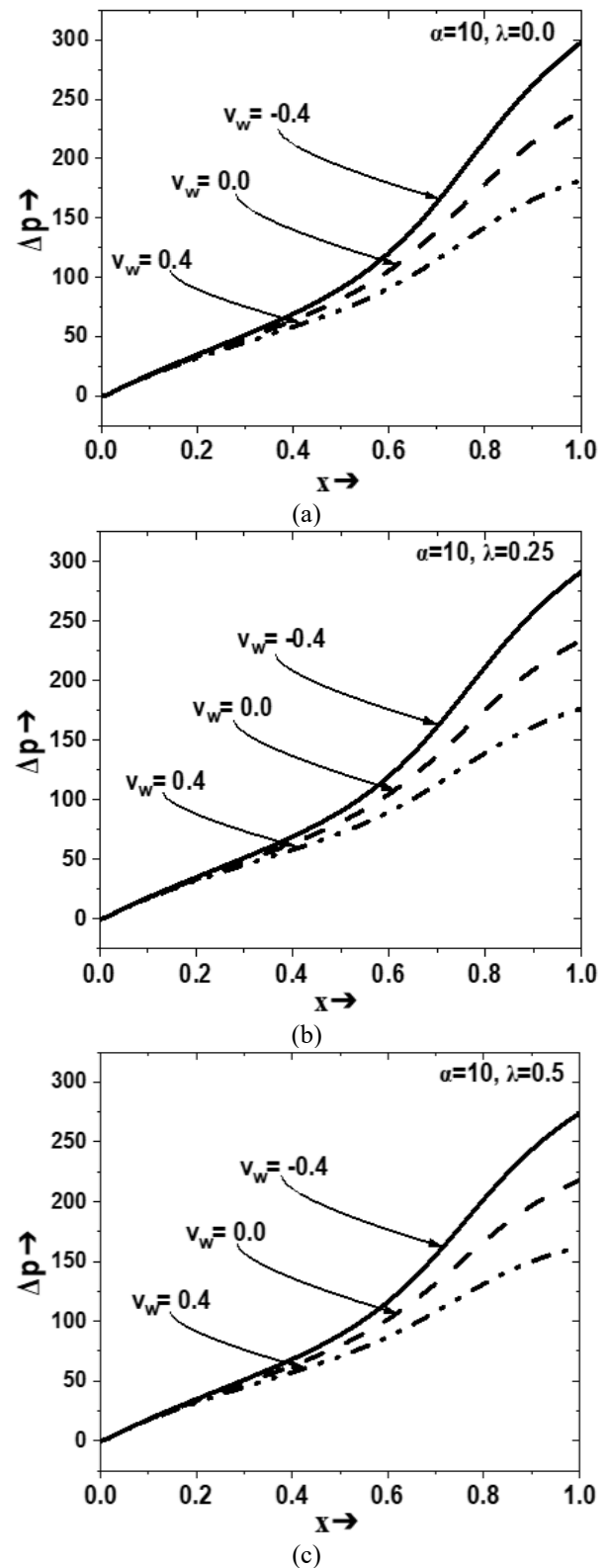
Figure 15. Δp vs. x for sinusoidal tube for $\alpha = 10$ in case of (a) λ =0, (b) λ =0.25, (c) λ =0.5

6. CONCLUSION

The present work examined the impact of suction/injection

velocity, elasticity parameter, and Womersley parameter on the mean pressure drop and wall shear stress modulus in an oscillatory flow of an elastic tube with suction/injection and varying cross-sections. Different geometries were taken into consideration. In our study, we linearized the non-linear governing equations using the perturbation method. This work makes an important contribution to our understanding of how suction/injection affects flow characteristics. An outline of the major findings of the work is provided below.

1. The aforementioned analysis has demonstrated that the geometry of the tube under study has an impact on the rise or fall in $|T_w|$ in addition to the parameters α and λ.

2. It is discovered that the suction causes the tube wall to endure less shear stress. Notably, the mean pressure drop for both rigid and elastic tube walls in the suction/injection scenario increases as the Womersley parameter increases.

3. Regardless of the geometry under consideration, the values of Δp decrease as the value of λ increases.

4. We investigated the dynamic relationship between suction/injection, oscillatory flow patterns, and tube wall elasticity using mathematical modeling. The outcomes shed light on the consequences of grasping blood flow dynamics in arteries with various geometries.

REFERENCES

[1] Fung, Y.C. (2013). Biomechanics: Circulation. Springer Science & Business Media. Springer, Singapore.

[2] Wautier, J.L., Wautier, M.P. (2022). Vascular permeability in diseases. International Journal of Molecular Sciences, 23(7): 3645. https://doi.org/10.3390/ijms23073645

[3] Womersley, J.R. (1955). Oscillatory motion of a viscous liquid in a thin-walled elastic tube—I: The linear approximation for long waves. The London, Edinburgh, and Dublin Philosophical Magazine and Journal of Science, 46(373): 199-221. https://doi.org/10.1080/14786440208520564

[4] Womersley, J.R. (1957). Oscillatory flow in arteries: The constrained elastic tube as a model of arterial flow and pulse transmission. Physics in Medicine and Biology, 2(2): 178-187. https://doi.org/10.1088/0031-9155/2/2/305

[5] Macey, R.I. (1963). Pressure flow patterns in a cylinder with reabsorbing walls. The Bulletin of Mathematical Biophysics, 25: 1-9. https://doi.org/10.1007/BF02477766

[6] Rao Ramachandra, A. (1983). Oscillatory flow in an elastic tube of variable cross-section. Acta Mechanica, 46: 155-165. https://doi.org/10.1007/BF01176771

[7] Chandra, P., Prasad, J.K. (1994). Pulsatile flow in circular tubes of varying cross-section with suction/injection. The ANZIAM Journal, 35(3): 366-381. https://doi.org/10.1017/S0334270000009358

[8] Chakravarty, S., Mandal, P.K. (2000). Two-dimensional blood flow through tapered arteries under stenotic conditions. International Journal of Non-Linear Mechanics, 35(5): 779-793. https://doi.org/10.1016/S0020-7462(99)00059-1

[9] Misra, J.C., Ghosh, S.K. (2003). Pulsatile flow of a viscous fluid through a porous elastic vessel of variable cross-section—A mathematical model for hemodynamic flows. Computers & Mathematics with Applications,

46(5-6): 947-957. https://doi.org/10.1016/S0898-1221(03)90155-6

[10] Das, K., Saha, G.C. (2012). Pulsatile motion of blood in a circular tube of varying cross-section with slip flow. International Journal of Engineering, Transactions B: Applications, 25: 9-18. https://doi.org/10.5829/idosi.ije.2012.25.01b.02

[11] Bhatti, K., Siddiqui, A.M., Bano, Z. (2017). Unsteady incompressible stokes flow through porous pipe of uniform circular cross section with periodic suction and injection. Sukkur IBA Journal of Computing and Mathematical Sciences, 1(1): 13-21. https://doi.org/10.30537/sjcms.v1i1.3

[12] Selvi, C.K., Srinivas, A.N.S. (2018). Oscillatory flow of a Casson fluid in an elastic tube with variable cross section. Applied Mathematics and Nonlinear Sciences, 3(2): 571-582. https://doi.org/10.2478/AMNS.2018.2.00044

[13] Gao, Y., Zhang, Z. (2020). Modelling and analysis of complex viscous fluid in thin elastic tubes. Complexity, 2020(1): 9256845. https://doi.org/10.1155/2020/9256845

[14] Manopoulos, C., Raptis, A., Tsangaris, S. (2022). Analytical solution of oscillatory stokes flow in a porous pipe with spatiotemporally periodic suction/injection. Applied Mechanics, 3(2): 683-691. https://doi.org/10.3390/applmech3020040

[15] Shahzad, A. (2022). Flow analysis in permeable channel with variable wall reabsorption. Waves in Random and Complex Media, pp. 1-19. https://doi.org/10.1080/17455030.2022.2148015

[16] Chaudhry, R., Miao, J.H., Rehman, A. (2022). Physiology, cardiovascular. StatPearls [Internet]. StatPearls Publishing, USA. https://www.ncbi.nlm.nih.gov/books/NBK493197/.

[17] Whitmore, R.L. (1968). Rheology of the Circulation. Pergamon Press, UK.

[18] Abramowitz, M., Stegun, I.A. (1948). Handbook of Mathematical Functions with Formulas, Graphs, and Mathematical Tables. US Government Printing Office.

NOMENCLATURE

U, V	Axial and radial components of velocity, LT^{-1}
P	Pressure, $ML^{-1}T^{-2}$
T	Time variable, T
V_w	Fluid velocity due to suction/injection, LT^{-1}
n	Frequency of oscillation, T^{-1}
A_0	Radius of the tube, L
L	The characteristic length of the tube, L
Q	Flow rate, L^3T^{-1}
τ_w	dimensional Wall shear stress, $ML^{-1}T^{-2}$
u, v	Dimensionless Axial and radial components of fluid's velocity
t	Dimensionless time variable
v_w	Dimensionless fluid velocity due to suction/injection
p	Dimensionless pressure
R_e	Dimensionless Reynolds number
S_t	Dimensionless Strouhal number
I_0, I_2	Modified Bessel functions of the first kind
T_w	Non dimensional Wall shear stress
Δp	Mean Pressure Drop

Greek symbols

ρ Fluid density, ML^{-3}
ν Kinematic viscosity, L^2T^{-1}
ζ Radial displacement, L
α Womersley number
σ Poisson's ratio

ε Slope parameter of the tube wall
λ Elasticity parameter
ξ Dimensionless radial displacement

Subscripts

0, 2   Order 0 and 2 respectively